



*Gen. Math. Notes, Vol. 32, No. 2, February 2016, pp. 80-104*

*ISSN 2219-7184; Copyright © ICSRS Publication, 2016*

*www.i-csrs.org*

*Available free online at <http://www.geman.in>*

# **Mixed Convection Radiating Flow and Heat Transfer in a Vertical Channel Partially Filled With a Darcy-Forchheimer Porous Substrate**

**A. Adeniyani<sup>1</sup> and I.A. Abioye<sup>2</sup>**

<sup>1</sup>Department of Mathematics, University of Lagos  
Akoka, Lagos, Nigeria

E-mail: [aadeniyani@unilag.edu.ng](mailto:aadeniyani@unilag.edu.ng)

<sup>2</sup>School of General Studies, Mathematics Department  
Maritime Academy of Nigeria, Oron, Akwa Ibom State, Nigeria

E-mail: [abioyeadesoye@yahoo.com](mailto:abioyeadesoye@yahoo.com)

(Received: 31-8-15 / Accepted: 11-1-16)

## **Abstract**

*In this study, an analysis has been carried out on mixed convection thermally radiating flow and heat transfer in a vertical channel partially filled with a Darcy-Forchheimer porous substrate of finite thickness attached to one of the walls taking into consideration the effects of permeability, Rosseland radiation and viscous dissipation. The governing equations have been reduced to non-linear ordinary differential equations by means of dimensional analysis and are solved analytically for some specific values of the non-dimensional governing flow parameters using Adomian Decomposition Method (ADM). The velocity and temperature profiles are assessed and discussed by means of graphs for various values of the pertinent emerging parameters. The shear stress parameters and the heat transfer rates at the walls as well as the velocity and temperature gradients are examined quantitatively. A comparison of the study has been made as a special case, with the more recent published work in the literature which lends itself to favorable agreement. It has been found that these emerging parameters have considerable influence on the flow and heat transfer characteristics.*

**Keywords:** *Adomian Decomposition Method, Darcy-Forchheimer, porous medium permeability, Rosseland radiation, viscosity coefficient, vertical walls.*

## 1 Introduction

The mixed convection or combined free-forced as a phenomenal mechanism, has its existence based on density changes or temperature differences for buoyancy related forces while forced convection may be sequel to the mechanized influence induced by an external agency such as flows maintained mechanically by pressure drop, mixer, agitator, fan blowing, etc. Nonetheless, the influence of thermal convective flow upwards along heated surfaces or downwards along cooled surfaces caused by buoyant forces is termed natural or free convection. On the other hand, that due to the influence of impressed forces such as pressure gradients and many related others is forced convection. Combined convection, a combination of natural and forced thermal convection with comparable order, in the presence of porous media is prevalent in a number of natural phenomena; and has varied wide range of many an engineering/industrial application as exemplified in enhanced extraction of crude oil, nuclear waste repositories, catalytic waste disposal, underground water management, filtration, heat exchangers, electronic devices, thermal insulation, packed bed catalytic reactors for removal of pollutants, oceanic and atmospheric circulations, extraction of geothermal energy, cooling of nuclear reactors, etc. A comprehensive list of several technological applications of this mechanism has been documented by Pop and Ingham [1], Nield and Bejan [2]. The analysis of free convective flow and heat transfer of a viscous fluid about a flat plate parallel to the direction of body forces with variable fluid properties and prescribed uniform wall temperature (PUWT) in a moving or an otherwise still viscous fluid was analyzed by Ostrach [3]. Beckermann et al. [4], who performed numerically and experimentally the steady-state natural convection fluid flow and heat transfer in a rectangular enclosure partially filled with a saturated porous medium. Hydrodynamic and heat transfer of a fully developed flow for a viscous and incompressible fluid streaming through a parallel-wall channel under various physical aspects with mixed convection effect has been studied extensively by many authors. Barletta [5] examined combined forced and free convection fully developed and viscously dissipating flow in a vertical parallel-plate channel with prescribed wall heat fluxes and obtained ordinary perturbation method (OPM) solutions. Chamkha [6] reported closed form solutions of velocity and temperature for mixed convection channel flow with symmetric and asymmetric wall heating conditions. Makinde and Osalusi [7] examined exactly the effect of magnetic field and wall-slip velocity on steady flow of an electrically conducting viscous fluid in a uniform width channel. Eegunjobi and Makinde [8] conducted a numerical investigation of entropy generation in a vertical porous channel through the effect of both buoyancy force and Navier slip and accessed solutions of both velocity and temperature using a shooting technique. Kamis et al. [9], of late, investigated through Buongiorno model the combined effects of variable viscosity and convective cooling on unsteady flow of nanofluids through a permeable pipe

using a semi-discretization finite difference method coupled with Runge-Kutta-Fehlberg scheme. Also, Adeniyani and Adigun [10] presented numerically the transient two-dimensional MHD boundary layer stagnation flow with heat and mass transfer in a saturated Darcian porous medium due to the simultaneous influence of pollutant concentration and the stress (pressure) work. Chauhan and Kumar [11] studied the effects of slip conditions on fully developed forced convection in a circular channel filled with a highly porous medium saturated with a rarefied gas and uniform wall surface heat flux, using Darcy extended Brinkman-Forchheimer model. Thermal radiation, an important mode of transference of heat energy owes its existence on a temperature power-law in the range of about 4 or 5 unlike thermal conduction and convection energy transfers which depend on difference in absolute temperatures approximately to the first power between two different locations in the flow regime, Siegel and Howell [12]. The influence of thermal radiation becomes very significant when the fluid density is low and working temperature is high. Several engineering and industrial processes such as high technology application in space shuttle, re-entry vehicles and solar power collectors, nuclear power plants, heat treatment of glass and metal plates, fibrous insulation, material surface coating and many others require heat energy transfer by radiation. Using the Rosseland approximation, Grosan and Pop [13] examined both analytically and numerically the thermal radiation effect on steady fully developed mixed convection flow in a vertical channel with different uniform wall temperatures. They observed a decrease in reversal flow with an increase in the radiation parameters. Most often it is necessary to introduce porous matrix into the flow regime in channel due to its ever demanding and increasingly important applications. Flows through porous media have several applications such as in agriculture engineering for curtailing excessive moisture that may damage farm food products such as permafrost degradation and undesirable high temperature of the soil and in petrochemical industries for filtration, adsorption and purification processes and environmental pollution management such as exhaust mufflers, to mention but a few. Israel-Cookey *et al.* [14] investigated the combined effects of radiative heat transfer and magnetic field on steady porous medium channel flow of an electrically conducting fluid with non-uniform wall temperatures. Chauhan and Rastogi [15] investigated natural convection MHD unsteady flow of a rotating viscous, thermally radiating and electrically conducting fluid in a vertical channel partially filled by a high porosity porous medium. Jain *et al.* [16] studied a free and forced convective slip flow, heat and mass transfer of a three dimensional viscous and incompressible fluid through a permeable vertical channel bounded by two vertical plates moving with equal velocity but in opposite directions. They observed that the skin friction coefficient is lower for water ( $Pr=7$ ,  $Sc=0.61$ ) than for air ( $Pr=0.71$ ,  $Sc=0.22$ ). Steady, laminar MHD flow of two immiscible viscous fluids with or without porous medium in the presence of heat generation was studied numerically by Chamkha [17]. Later on, Salah El-Din [18, 19], in the first of the two papers discussed analytically the effect of viscous dissipation on fully developed laminar mixed convection flow in a horizontal double passage channel and later extended in the second paper with inclusion of buoyancy forces as per vertical channel and obtained numerical solutions. The results show significant influence of the baffle

position on the pertinent flow and heat transfer characteristics. Sastry et al. [20] investigated exactly the Couette flow of two immiscible viscous fluids between two permeable horizontal beds using Darcy's law for the upper bed and Brinkman's for the lower. Several authors have investigated various physical aspects of the transient oscillatory fluid flow through a channel filled with a saturated porous medium, to mention but a few, Makinde and Mhone [21], Hamza et al. [22], Adesanya and Makinde [23] all obtained closed-form analytical solutions. Chauhan and Agrawal [24] analyzed numerically in the first paper using Crank-Nicolson scheme, the MHD coupled slip flow of Newtonian fluid past an infinite horizontal plate at the bottom of a porous finite thickness layer whilst in the second use was made of homotopy analysis method (HAM) to analyze the MHD flow of viscous electrically conducting fluid between a porous medium bed and a shrinking sheet. Narahari [25] investigated analytically the transient free convection flow of a viscous and incompressible fluid between two infinite vertical parallel plates in the presence of constant wall temperature and mass diffusion whilst solution accessed by Laplace transform method. Rajput and Sahu [26, 27], presented the transient free convective MHD flow streaming between two infinite vertical parallel plates with constant wall temperature and mass diffusion, and thermal radiation in their first paper whilst the second is without radiation effect though with variable wall temperature and uniform mass diffusion. Use was made of the Laplace transform method in the latter while a combination of analytic/numerical technique invoked in the former. Singh [28] studied thermal radiation with MHD mixed convection visco-elastic slip flow through a porous medium in a vertical porous channel. Chauhan and Kumar [29] examined a fully developed mixed convection viscous fluid flow between two infinite vertical parallel plane walls, where a porous substrate of finite thickness is attached to the left vertical wall in the presence of radiation and viscous dissipation effects using the ordinary perturbation method (OPM) for the dimensionless fluid velocity and temperature fields. Adomian decomposition method (ADM), an approximate series solution proposed by Adomian [30] has been found efficient and strongly promising for tackling a wide range of boundary value problems (BVPs) in engineering and sciences. This method, unlike the traditional perturbation method is free of restrictions and limitations of largeness/smallness of selected flow parameter and it is expected to proffer more reliable analytical results. The convergence of the series may be powered or enhanced by Padé approximants to accelerate the convergence of ADM series. Several researchers Wazwaz et al. [31], Mirgolbabaie et al. [32], Noor et al. [33], Makinde et al. [34, 35], Heidarzadeh et al. [36] among others in the recent past, successfully employed the method to solve nonlinear BVPs. More recently, Kumar et al. [37] analyzed free and forced convective flow in a vertical channel filled with composite porous medium with Darcy dissipation and Robin boundary conditions using Darcy-Lapwood-Brinkman model. They accessed analytical solutions via the ordinary perturbation method (OPM) and differential transform method (DTM). Studies conducted by Bellomo and Monaco [38] and Rach [39] respectively indicated significant merits of ADM over the perturbation technique and Picard's method for finding solutions of some scientific problems with

nonlinear nature. Saleh and Hashim [40], who focused on flow reversal phenomena for MHD mixed convection in a vertical channel, however employed shooting technique.

In all the literature survey discussed in the aforementioned studies, one notices that none considered the influence of porous medium permeability due to the quadratic variation in the fluid velocity. Since moderately strong fluid velocity in saturated porous medium is associated with many flow and heat transfer problems in the context of laminar viscous flow streaming through the channels; and most especially those in which a porous substrate is attached to channel wall, it would be of interest and importance to include the joint effects of viscous dissipation, viscous heating, Darcy-Forchheimer quadrature on thermally radiating viscous and incompressible fully developed hydrodynamic flow through a parallel vertical wall channel. This aspect forms the subject matter of the present communication which may be regarded as an extension of Ref. [29] besides the ADM adopted for the solutions of the resulting dimensionless boundary value problems (BVPs).

## 2 Mathematical Formulation

Consider steady two dimensional laminar, fully developed flow of a viscous fluid streaming through the region between two infinitely long vertical parallel plates in which a finitely thick Darcy-Forchheimer substrate of uniform porous permeability has been bonded perfectly with the left wall of the channel as depicted in the schematic diagram of Fig.1. The channel width or hydraulic diameter is  $D$  while the substrate slab thickness is  $h$ . The  $\bar{x}$  – axis coincides with the left plate and extends in the reverse direction to that of the acceleration due to gravity; such that  $-\infty < \bar{x} < \infty$  while the  $\bar{y}$  – axis is taken perpendicular to the channel parallel plates.

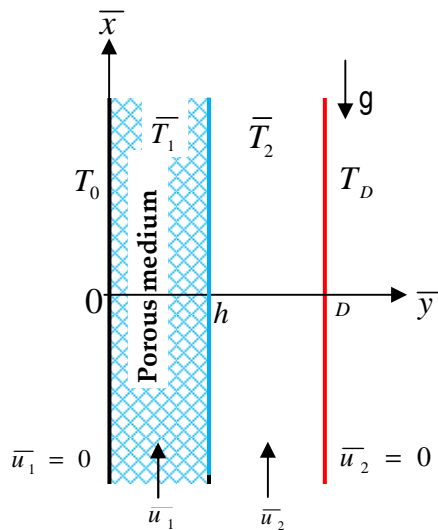


**Fig. 1:** Schematic diagram

Another axis on the plane intersecting orthogonally with the  $\bar{x}$  – axis along which there is neither convection current nor stream-flow also extends without bounds. It is assumed that the left plate through the origin O and the right plate through D have prescribed uniform wall temperatures  $T_0$  and  $T_D$  respectively; satisfying  $T_D > T_0$ . Further it shall be assumed that both the porous medium of the substrate slab and the flowing fluid are thermally in equilibrium at every location. Under fully developed flow approximation, the fluid velocity is described by components  $\bar{u}_i, \bar{v}_i$  along  $\bar{x}, \bar{y}$  respectively such that the subscripts  $i = 1, 2$  connote the porous substrate slab or porous region ( $0 \leq \bar{y} \leq h$ ) and substrate-free or clear fluid region ( $h \leq \bar{y} \leq D$ ) of the flow regime. In this model, we assume the usual Boussinesq approximation that all fluid properties remain constant except the variation of the fluid density in the body-force term only in the Naviers-Stokes equations. Therefore, the fluid densities in both substrate slab and substrate-free regions may be posited approximately as

$$\rho = \rho_0[1 - \beta(\bar{T}_i - T_m)], i = 1, 2 \quad (1)$$

for first order approximation of Taylor series expansion about the reference density  $\rho_0$ . In line with full discussion on the choice of fluid temperature for fully-established mixed convection channel flow Barletta and Zanchini [41].

$T_m = \frac{T_0 + T_D}{2}$ , the mean temperature of the channel wall temperatures signifies the reference temperature,  $\beta$  is the thermal expansion coefficient,  $\bar{T}_1$  and  $\bar{T}_2$  are fully developed fluid temperatures in substrate slab and substrate-free regions respectively. In order to address the influence of thermal radiation for this present channel flow model, use will be made of the Roseland approximation Ref. [12], neglecting the radiative heat flux in the  $\bar{x}$  direction, the dominant radiative heat flux along the  $\bar{y}$  direction discerningly takes the form

$$\bar{q}_r = -\frac{4\sigma^*}{3k^*} \frac{\partial \bar{T}_1^4}{\partial \bar{y}}, \quad q_r = -\frac{4\sigma^*}{3k^*} \frac{\partial \bar{T}_2^4}{\partial \bar{y}} \quad (2)$$

for an optically thin viscous hydrodynamic fluid flowing through the channel.

Where  $\sigma^*$  and  $k^*$  are the Stefan-Boltzmann constant and the mean absorption coefficient for thermal radiation.

Essentially, the use of Taylor's theorem for the expansion of temperature dependent function  $F(\bar{T}_i) = \bar{T}_i^4$  about the fluid mean or reference temperature  $T_m$ , lends itself to the smallness of temperature difference  $\bar{T}_i - T_m$ . Consequently

$$\bar{T}_i^4 = \bar{T}_m^4 + 4(\bar{T}_i - T_m)\bar{T}_m^3 + 6(\bar{T}_i - T_m)^2\bar{T}_m^3 + \dots \quad (3)$$

and on neglecting higher order terms, one obtains

$$\bar{T}_i^4 \approx T_m^3(4\bar{T}_i - 3T_m), \quad (i = 1, 2). \quad (4)$$

Using this (4) discerningly in the set of eqns. (2), we find

$$q_r = -\frac{16\sigma^*T_m^3}{3k^*} \frac{\partial \bar{T}_1}{\partial \bar{y}}, \quad \frac{\partial q_r}{\partial \bar{y}} = -\frac{16\sigma^*T_m^3}{3k^*} \frac{\partial^2 \bar{T}_2}{\partial \bar{y}^2}. \quad (5)$$

Taking into cognizance all the assumptions stated earlier, therefore the equations of mass conservation, momentum and energy balance for the Newtonian fluid model in the two regions are posited as

$$\frac{\partial \bar{u}_i}{\partial \bar{x}} + \frac{\partial \bar{v}_i}{\partial \bar{y}} = 0, \quad i = 1, 2 \quad (6)$$

$$\bar{u}_1 \frac{\partial \bar{u}_1}{\partial \bar{x}} + \bar{v}_1 \frac{\partial \bar{u}_1}{\partial \bar{y}} = -\frac{1}{\rho_0} \frac{\partial p}{\partial \bar{x}} + \frac{\bar{\mu}}{\rho_0} \frac{\partial^2 \bar{u}_1}{\partial \bar{y}^2} + g\beta(\bar{T}_1 - T_m) - \frac{\mu}{\rho_0 K} \bar{u}_1 - \frac{b_F \rho_0 u_0}{\mu \sigma^2} \bar{u}_1^2 \quad (7)$$

$$\bar{u}_2 \frac{\partial \bar{u}_2}{\partial \bar{x}} + \bar{v}_2 \frac{\partial \bar{u}_2}{\partial \bar{y}} = -\frac{1}{\rho_0} \frac{\partial p}{\partial \bar{x}} + \frac{\mu}{\rho_0} \frac{\partial^2 \bar{u}_2}{\partial \bar{y}^2} + g\beta(\bar{T}_2 - T_m) \quad (8)$$

$$\rho_0 C_p \left( \bar{u}_1 \frac{\partial \bar{T}_1}{\partial \bar{x}} + \bar{v}_1 \frac{\partial \bar{T}_1}{\partial \bar{y}} \right) = \bar{k} \frac{\partial^2 \bar{T}_1}{\partial \bar{y}^2} - \frac{\partial \bar{q}_r}{\partial \bar{y}} + \bar{\mu} \left( \frac{\partial \bar{u}_1}{\partial \bar{y}} \right)^2 + \frac{\mu}{K} \bar{u}_1^2 \quad (9)$$

$$\rho_0 C_p \left( \bar{u}_2 \frac{\partial \bar{T}_2}{\partial \bar{x}} + \bar{v}_2 \frac{\partial \bar{T}_2}{\partial \bar{y}} \right) = k \frac{\partial^2 \bar{T}_2}{\partial \bar{y}^2} - \frac{\partial q_r}{\partial \bar{y}} + \mu \left( \frac{\partial \bar{u}_2}{\partial \bar{y}} \right)^2 \quad (10)$$

$$\frac{\partial p}{\partial \bar{y}} = 0 \quad (11)$$

with the accompanying boundary and matching interface conditions Ref. [29]:

$$\bar{u}_1(0) = 0, \bar{T}_1(0) = T_0, \bar{u}_2(D) = 0, \bar{T}_2(D) = T_D \quad (12a)$$

$$\bar{u}_1(h) = \bar{u}_2(h), \bar{T}_1(h) = \bar{T}_2(h), \bar{\mu} \frac{\partial \bar{u}_1}{\partial \bar{y}}(h) = \mu \frac{\partial \bar{u}_2}{\partial \bar{y}}(h), \bar{k} \frac{\partial \bar{T}_1}{\partial \bar{y}}(h) = k \frac{\partial \bar{T}_2}{\partial \bar{y}}(h) \quad (12b)$$

where,  $C_p$  is the specific heat at constant pressure and  $K$  is the permeability of the porous medium,  $k$  is the thermal conductivity,  $\bar{k}$  effective thermal conductivity in the porous medium,  $\mu$  is the viscosity of the clear fluid,  $\bar{\mu}$  is the effective viscosity of the fluid in porous medium,  $g$  is the acceleration due to gravity,  $\nu$  is the kinematic viscosity; where  $\mu = \rho_0 \nu$ . In addition, the Forchheimer coefficient is designated by  $b_F$ .

It is importantly necessary to highlight further assumptions invoked into this present channel flow model through eqns. (12a) - (12b). Specifically, the usual no-slip velocity conditions at the channel walls and very different wall temperatures have been presumed as presented in (12a) while equality in fluid

velocities, temperatures, shear stresses and thermal fluxes across the porous-substrate and substrate-free interface are unveiled by (12b).

As the channel is infinitely long, the entrance correction can be ignored so that fully developed flow guarantees that the velocity components  $v_i = 0$ , ( $i = 1, 2$ ). Under this claim, the equation of conservation of mass (6) reduces to  $\frac{\partial \bar{u}_i}{\partial \bar{x}} = 0$  which integrates to give  $\bar{u}_i = \bar{u}_i(\bar{y})$ , a function of  $\bar{y}$  only; while the  $\bar{y}$ -component of the momentum balance equation (11) automatically simplifies to give  $\frac{\partial p}{\partial \bar{x}}$  as a constant or  $p = p(\bar{x})$  a function of  $\bar{x}$  only. In summary we may write

$$p = p(\bar{x}), v_i = 0, \frac{\partial \bar{u}_i}{\partial \bar{x}} = 0, \bar{u}_i = \bar{u}_i(\bar{y}), (i = 1, 2). \quad (13)$$

For convenience, one may nondimensionalize the remaining governing equations alongside the boundary and matching interface conditions by the following parameters:

$$x = \frac{\bar{x}}{D}, y = \frac{\bar{y}}{D}, u_i = \frac{\bar{u}_i}{u_0}, T_i = \frac{\bar{T}_i - T_m}{T_D - T_0}, (i = 1, 2). \quad (14)$$

Following Ref. [6, 29, 40] the pressure gradient and the reference velocity are

$$\frac{dp}{d\bar{x}} = -A, u_0 = \frac{AD^2}{48\mu}. \quad (15)$$

Substitution of eqns. (13) and (15) into eqns. (6) through (10) gives rise to the following eqns:

### Region-I (Porous Substrate Slab)

$$\frac{A}{\rho_0} + \frac{\bar{\mu}}{\rho_0} \frac{\partial^2 \bar{u}_1}{\partial \bar{y}^2} + g\beta(\bar{T}_1 - T_m) - \frac{\nu}{K} \bar{u}_1 - \frac{b_F u_0}{\nu \sigma^2} \bar{u}_1^2 = 0 \quad (16)$$

$$\frac{\bar{k}}{\rho_0 c_p} \frac{\partial^2 \bar{T}_1}{\partial \bar{y}^2} - \frac{1}{\rho_0 c_p} \frac{\partial \bar{q}_r}{\partial \bar{y}} + \frac{\bar{\mu}}{\rho_0 c_p} \left( \frac{\partial \bar{u}_1}{\partial \bar{y}} \right)^2 + \frac{\nu}{K c_p} \bar{u}_1^2 = 0 \quad (17)$$

### Region-II (Substrate-Free or Clear Fluid)

$$\frac{A}{\rho_0} + \nu \frac{\partial^2 \bar{u}_2}{\partial \bar{y}^2} + g\beta(\bar{T}_2 - T_m) = 0 \quad (18)$$

$$\frac{k}{\rho_0 c_p} \frac{\partial^2 \bar{T}_2}{\partial \bar{y}^2} - \frac{1}{\rho_0 c_p} \frac{\partial q_r}{\partial \bar{y}} + \frac{\nu}{K c_p} \left( \frac{\partial \bar{u}_2}{\partial \bar{y}} \right)^2 = 0 \quad (19)$$

Invoking the boundary condition (12a) on eqns. (16) and (18), replacing the effective viscosity  $\bar{\mu}$  by  $\mu\phi_1$  and simplifying to have the following set of derived boundary conditions:

$$\left. \frac{d^2\bar{u}_1}{dy^2} \right|_{y=0} = -\frac{A}{\mu\phi_1} - \frac{g\beta(\bar{T}_1 - T_m)}{v\phi_1}, \quad \left. \frac{d^2\bar{u}_2}{dy^2} \right|_{y=D} = -\frac{A}{\mu} - \frac{g\beta(\bar{T}_1 - T_m)}{v} \quad (20)$$

where  $\phi_1 = \frac{\bar{\mu}}{\mu}$  is the viscosity ratio.

Using (4) in (5), transferring the results into the energy balance eqns. (17) and (19), and then nondimensionalize with (14) the resulting energy eqns. along with the momentum balance eqns. (16) and (18), simplifying discerningly to obtain

$$T_1 = -\frac{1}{\lambda} [48 + \phi_1 u_1'' - \sigma^2 u_1 - \sigma^2 F_s u_1^2] \quad (21)$$

$$T_1'' = -\frac{3N\phi_1 Br}{3N\phi_2 + 4} (u_1')^2 - \frac{3N\sigma^2 Br}{3N\phi_2 + 4} u_1^2 \quad (22)$$

$$T_2 = -\frac{1}{\lambda} (48 + u_2'') \quad (23)$$

$$T_2'' = -\frac{3NBr}{3N + 4} (u_2')^2 \quad (24)$$

Where

$$\left. \begin{aligned} \phi_2 &= \frac{\bar{k}}{k}, & \sigma &= \frac{D}{\sqrt{k_0}}, & F_s &= \frac{u_0 b_f}{v}, & Re &= \frac{u_0 D}{v}, \\ Br &= \frac{\mu u_0^2}{k(T_1 - T_2)}, & Gr &= \frac{g\beta(T_D - T_0)D^3}{v^2}, & N &= \frac{kk^*}{4\sigma^* T_m^3}, & \lambda &= \frac{Gr}{Re} \end{aligned} \right\} \quad (25)$$

are respectively thermal conductivity ratio, permeability parameter (or Darcy number), Forchheimer number, Reynolds number, Brinkman number, mixed convection parameter, Stark number (or conduction-radiation parameter) and mixed convection parameter (or modified Grashof number).

Twice differentiating  $T_1$  in (21) with respect to  $y$ ; and substituting the result into (22), repeating the same for  $T_2$  in (23) for use in (24) and after a rearrangement of terms and simplification, one obtains the following set of fourth order nonlinear ODEs:

$$u_1^{(iv)} = K_2(1 + 2F_s u_1)u_1'' + (K_1 + 2K_2 F_s)(u_1')^2 + K_1 K_2 u_1^2 \quad (26)$$

$$u_2^{(iv)} = K_3(u_2')^2 \quad (27)$$

Where

$$K_1 = \frac{3N\lambda Br}{3N\phi_2 + 4}, \quad K_2 = \frac{\sigma^2}{\phi_1}, \quad K_3 = \frac{3N\lambda Br}{3N + 4} \quad (28)$$

Further, the nondimensional boundary and matched interface conditions are derived by utilizing eqn. (14) in (12a) –(12b) and (21), and written as

$$u_1(0) = 0, T_1(0) = -\frac{1}{2}, \quad u_1''(0) = \frac{48}{\phi_1} + \frac{\lambda}{2\phi_1} \quad (29a)$$

$$u_2(1) = 0, T_2(1) = \frac{1}{2}, \quad u_2''(1) = -48 - \frac{\lambda}{2} \quad (29b)$$

$$\left. \begin{aligned} u_1(a) = u_2(a), T_1(a) = T_2(a), \phi_1 u_1''(a) - \sigma^2 u_1(a) = u_2''(a), \\ \phi_1 u_1'(a) = u_2'(a), \phi_2 (u_1'''(a) - \sigma^2 u_1'(a)) = u_2'''(a) \end{aligned} \right\} \quad (29c)$$

The pertinent engineering quantities of interest are the skin-friction coefficients and the Nusselt numbers. These quantities may be stated respectively in terms of the wall shear stresses and the surface heat fluxes as:

$$C_{f_i} = \frac{\tau_{wi}}{\rho_0 U_0^2}, \quad Nu_i = \frac{Dq_{wi}}{k(T_D - T_m)}, \quad (i = 1, 2) \quad (30)$$

Where

$$\tau_{w1} = \bar{\mu} \left. \frac{\partial \bar{u}_1}{\partial \bar{y}} \right|_{\bar{y}=0}, \quad \tau_{w2} = \mu \left. \frac{\partial \bar{u}_2}{\partial \bar{y}} \right|_{\bar{y}=1}, \quad q_{w1} = -\bar{k} \left. \frac{\partial \bar{T}_1}{\partial \bar{y}} \right|_{\bar{y}}, \quad q_{w2} = -k \left. \frac{\partial \bar{T}_2}{\partial \bar{y}} \right|_{\bar{y}=1} \quad (31)$$

They are transformed by (14) to yield their respective nondimensional forms written as

$$C'_f(0) = C_{f_1} \text{Re} = \phi_1 u_1'(0), \quad C'_f(1) = C_{f_2} \text{Re} = u_2'(1), \quad Nu'(0) = -\phi_2 T_1'(0), \quad Nu'(1) = -T_2'(1) \quad (32)$$

### 3 Solution Methods

#### 3.1 Some Important Cases

##### 3.1.1 Negligible Forchheimer Number

The situation where the effect of Forchheimer permeability is inconsequential is frequently associated with slowly streaming flow in a region constrained by the parallel channel walls. In which case,  $F_s = 0$  in this present work lends itself to the equations reported by Ref. [29].

##### Pure Forced Convection ( $\lambda = 0$ )

In the case of purely forced convection, when the free or natural convection effect is inconsequential, then  $\lambda = 0$  implying that  $K_1 = K_3 = 0$ . Eqns. (26) and (27) reduce to

$$u_1^{(iv)} = K_2 \left[ (1 + 2F_s u_1) u'' + 2K_2 F_s (u_1')^2 \right] \quad (33)$$

$$u_2^{(iv)} = 0 \quad (34)$$

Although (33) still retains its nonlinearity nature, fortunately (34) integrates completely to yield

$$u_2 = c_0 + c_1 y + c_2 y^2 + c_3 y^3 \quad (35)$$

wherein the constants  $c$ 's are determined under the present circumstance, ignoring the buoyancy parameter in the boundary conditions (29a-c). The dimensionless temperature field  $T_1$  in the porous substrate region-I, using (35) in (27), can thusly be evaluated. If however,  $F_s=0$  is imposed in (33), then

$$u_1^{(iv)} = K_2 u'' \quad (36)$$

with the general solution

$$u_1 = a_0 + a_1 y + a_3 \sin \omega y + a_4 \cosh \omega y \quad (37)$$

where  $a$ 's are constants that can be determined by means of the boundary conditions (29a-c) and

$$\omega = \sqrt{K_2}$$

### 3.1.2 Predominant Conduction-Radiation ( $N \rightarrow \infty$ )

The case for which the conduction-radiation parameter  $N$  is finitely large,  $K_1 \rightarrow \lambda Br / \phi_2$ ,  $K_3 \rightarrow \lambda Br$  so that (26) and (27) take the form

$$\begin{aligned} u_1^{(iv)} &= K_2 (1 + 2F_s u_1) u_1'' + (K_1 + 2K_2 F_s) (u_1')^2 + K_1 K_2 u_1^2 \\ u_2^{(iv)} &= K_3 (u_2')^2 \end{aligned} \quad (38)$$

In this special case, the resulting BVPs (26)-(28), (29a-b) are nonlinear.

### 3.1.3 Infinitely Large Viscosity and/or Thermal Conductivity Ratios ( $\phi_1, \phi_2 \rightarrow \infty$ )

The special case wherein the viscosity ratio and/or the thermal conductivity ratio are infinite in values, proffers the same solution as presented in section (3.1.2) above. That is, ( $\phi_1 \rightarrow \infty$  and  $\phi_2 \rightarrow \infty$ ), ( $\phi_1 \rightarrow \infty$  or  $\phi_2 \rightarrow \infty$ ).

## 3.2 Adomian Decomposition Method

Adopting the standard decomposition procedure proposed by Ref. [30], we introduce linear differential operator and its inverse:

$$L_y^4 = \frac{d^4}{dy^4}, \quad L_y^{-4}(\bullet) = \int_0^y \int_0^y \int_0^y \int_0^y (\bullet) d\eta d\eta d\eta d\eta \quad (39)$$

It may be convenient to rearrange eqns. (24) through (25) using (26) in operational forms as follows

$$L_y^4 u_i = g_i(y) - Ru_i - N(u_i) \quad (i=1,2) \quad (40)$$

where the LHS of (40) denotes the highest order derivative,  $g_i(y)$  is the source function,  $Ru_i$  is the remainder of the linear term with derivative order less than 4, while  $N(u_i)$  are nonlinear terms:

$$N(u_1) = 2K_2 F_s u_1 u_1'' + (K_1 + 2K_2 F_s) (u_1')^2 + K_1 K_2 u_1^2, \quad Ru_1 = K_2 u_1'' \quad (41a)$$

$$N(u_2) = K_3 (u_2')^2, \quad Ru_2 = g = 0 \quad (41b)$$

which may be represented by infinite series of the so-called Adomian polynomials

$A_n$ ,  $B_n$ ,  $C_n$  and  $D_n$  as:

$$\sum_{n=0}^{\infty} A_n = U_n U_n'', \quad \sum_{n=0}^{\infty} B_n = (U_n')^2, \quad \sum_{n=0}^{\infty} C_n = (U_n)^2 \text{ and } \sum_{n=0}^{\infty} D_n = (V_n')^2 \quad (42a)$$

$$A_n = \frac{1}{n!} \left\{ \frac{d^n}{d\xi^n} \left[ F \left( \sum_{i=0}^n \xi^i U_i \right) \right] \right\}_{\xi=0}, \quad (42b)$$

such that  $B_n$ ,  $C_n$  and  $D_n$  are specified as  $A_n$  in (41b) for  $n = 0, 1, 2, \dots$  and more importantly  $\xi$  is a parameter introduced for convenience for  $n=0, 1, 2, \dots$  and in addition we have replaced  $u_1$  by  $U$  and  $u_2$  by  $V$ .

Applying the inverse operator on eqns. (26)-(27), one obtains

$$\begin{aligned} U(y) = & U(0) + U'(0)y + U''(0)\frac{y^2}{2} + U'''(0)\frac{y^3}{6} + L_y^{-4} [K_2 U''] + L_y^{-4} [2K_2 F_s U U''] \\ & + L_y^{-4} [(K_1 + 2K_2 F_s)(U')^2] + L_y^{-4} [K_1 K_2 U^2] \end{aligned} \quad (43)$$

$$V(y) = V(0) + yV'(0) + \frac{y^2}{2}V''(0) + \frac{y^3}{6}V'''(0) + L_y^{-4} [K_2 V^2] \quad (44)$$

More importantly, the general solutions proffered by ADM are the infinite series Hasan and Zhu [42]

$$U = \sum_{n=0}^{\infty} U_n, \quad V = \sum_{n=0}^{\infty} V_n \text{ along with N-th partial sums } \Phi_N = \sum_{n=0}^{N-1} U_n, \quad \Psi_N = \sum_{n=0}^{N-1} V_n$$

where the n-terms ( $U_n, V_n$ ) are determined recursively and the N-th partial sums can be used to access the approximate exact solutions iteratively depending on the degree of accuracy so desired.

If  $(u_1, u_2)$  are replaced by  $(U, V)$  and  $K_1, K_2, K_3$  substituted for, by means of (38) the computation algorithm can be started off as follows:

$$U_0 = \alpha_1 y + \left[ -\frac{48}{\phi_1} + \frac{\lambda}{2\phi_1} \right] \frac{y^2}{2} + \alpha_2 \frac{y^3}{6} \quad (45)$$

$$V_0 = \alpha_3 + \alpha_4 y + \frac{1}{2} \alpha_5 y^2 + \frac{1}{6} \alpha_6 y^3. \quad (46)$$

Where

$$\alpha_1 = U'(0), \alpha_2 = U''(0), \alpha_3 = V(0), \alpha_4 = V'(0), \alpha_5 = V''(0), \alpha_6 = V'''(0) \tag{47}$$

are unspecified boundary conditions whose values will be determined on using eqns. (29a-c) and

for  $n \geq 1$ , the recursive relation takes the form

$$U_{n+1}(y) = U_n(0) + U'_n(0)y + U''_n(0)\frac{y^2}{2} + U'''_n(0)\frac{y^3}{6} + \frac{\sigma^2}{\phi_1} L_y^4 [U''_n] + 2\frac{\sigma^2}{\phi_1} F_s L_y^4 [U_n U''_n] + \left( \frac{\lambda Br}{\phi_2} + 2\frac{\sigma^2}{\phi_1} F_s \right) L_y^4 [(U'_n)^2] + \frac{\lambda Br}{\phi_2} \frac{\sigma^2}{\phi_1} L_y^4 [U_n^2] \tag{48}$$

$$V_{n+1}(y) = V_n(0) + yV'_n(0) + \frac{y^2}{2} V''_n(0) + \frac{y^3}{6} V'''_n(0) + \frac{\lambda Br}{\phi_2} L_y^4 [V_n^2]. \tag{49}$$

The set of equations (45) through (49) encompassed by the algorithm has been coded in computer algebraic language using Maple-18 software package for simulations system of equations and then implemented for parametric values of the emerging flow parameters. It is worthy to mention that the task of evaluating the unspecified parameters is very challenging. Nonetheless, the substitutions of (47) into our approximated exact solutions of U and V, assisted by coded program for simultaneous system of equations lend themselves to the much needed boundary conditions.

## 4 Results and Discussion

### 4.1 Tabular Results

**Table 1:** Computations showing the results of variation of each dimensionless parameter

$F_s$	$Br$	$\sigma$	$Gr$	$a$	$\phi_2$	$\phi_1$	$N$	$C_f'(0)$	$C_f'(1)$	$Nu'(0)$	$Nu'(1)$
5	0.1	1	1	0.2	1.67	1.25	1	25.06369215	-26.80088570	4.407405645	-18.33788094
10	0.1	1	1	0.2	1.67	1.25	1	22.60273600	-24.69932556	4.440950002	-18.34064064
15	0.1	1	1	0.2	1.67	1.25	1	19.62407696	-22.47055555	4.490118062	-18.35247201
5	0.1	1	1	0.2	1.67	1.25	1	25.06369220	-26.80088573	4.407405643	-18.33788093
5	0.2	1	1	0.2	1.67	1.25	1	25.34430791	-27.09682689	8.702375526	-41.09393358
5	0.5	1	1	0.2	1.67	1.25	1	26.27435581	-28.08205469	27.65028150	-146.1121504
5	0.1	1	1	0.2	1.67	1.25	1	25.06369213	-26.80088569	4.407405658	-18.33788094
5	0.1	3	1	0.2	1.67	1.25	1	12.63074708	-26.80088569	5.94572559	-18.55222718

5	0.1	5	1	0.2	1.67	1.25	1	8.236682860	-15.59976034	15.38221685	-20.64771733
5	0.1	1	1	0.2	1.67	1.25	1	25.06369215	-26.80088570	4.407405688	-18.33788094
5	0.1	1	3	0.2	1.67	1.25	1	25.54144270	-27.60712940	4.944551513	-21.84308128
5	0.1	1	5	0.2	1.67	1.25	1	26.09243505	-28.49245308	5.847235174	-27.58771449
5	0.1	1	1	0.1	1.67	1.25	1	25.06369216	-26.80088571	5.112910441	-22.11381132
5	0.1	1	1	0.2	1.67	1.25	1	13.59388778	-17.04334189	4.407405672	-18.33788094
5	0.1	1	1	0.3	1.67	1.25	1	11.24412289	-13.73877226	3.988639742	-15.09554123
5	0.1	1	1	0.2	1.00	1.25	1	24.68857697	-26.53177169	6.827805054	-19.17620205
5	0.1	1	1	0.2	1.25	1.25	1	24.86774897	-26.66027339	5.664992681	-18.77316570
5	0.1	1	1	0.2	1.67	1.25	1	25.06369217	-26.80088572	4.407405670	-18.33788093
5	0.1	1	1	0.2	1.67	0.2	1	34.26510774	-18.40454854	4.909321291	-18.44310908
5	0.1	3	1	0.2	1.67	0.4	1	32.18819185	-21.12470481	4.438061881	-18.33638321
5	0.1	5	1	0.2	1.67	0.6	1	31.67136451	-23.58843581	4.392925724	-18.34031768
5	0.1	1	1	0.2	1.67	1.25	10	8.960610322	-42.55543785	25.33772588	-27.09947642
5	0.1	1	1	0.2	1.67	1.25	30	9.788189089	-47.01314704	25.38293091	-27.14939391
5	0.1	1	1	0.2	1.67	1.25	50	9.974139451	-48.01698689	25.39291752	-27.16044228

The responses of the skin-friction coefficients and the Nusselt numbers due to variations in the basic governing flow parameters are unveiled in Table 1. As observed, the skin-friction parameters intensify absolutely in values for both hot and cold parallel plates when Brinkman number  $Br$ , Grashof number  $Gr$ , conductivity ratio  $\phi_2$  and Forchheimer number  $Fs$ , in the range  $0.01 \leq Fs \leq 0.03$  strengthen in values but all diminish absolutely as not only  $Fs$  in the larger range  $5 \leq Fs \leq 15$  but also substrate thickness parameter improve in value. Both wall surface shear parameters  $C'_f(0)$  and  $C'_f(1)$  reduce absolutely as the permeability parameter  $\sigma$  intensifies. On the other hand, the heat transfer rates at the walls increase with  $\sigma$ ,  $Br$  and  $Gr$ . The Nusselt numbers  $Nu'(0)$  and  $Nu'(1)$ , and skin-friction coefficients all reduce values as the permeability ratio  $\phi_1$  increases while all  $C'_f(0)$ ,  $C'_f(1)$ ,  $Nu'(0)$  and  $Nu'(1)$  can be increased due to intensification of the radiation parameter  $N$ .

## 4.2 Graphical Results

The comparison in the velocity profiles between the parametric perturbation method (PPM) and the Adomian decomposition method (ADM) is displayed in Figure 2. As it can be seen, there appears to be little deviation in the plots due to the two methods. However, the merit of using approximate analytic method over the usual assumption of smallness in perturbation parameter has been found advantageous besides the accompanying insuperable mathematical difficulties. Figures 3-4 demonstrate the velocity profiles for varying legend parameters  $Fs$  and the substrate thickness  $a$ , for which each profile increases from the zero wall value with a kink at the fluid-substrate interface and then progressively continues until a peak value is attained at about the centerline after which it sequentially loses values in the clear fluid region to stick to the hot plate, again with zero velocity. The plots as revealed in Figures 5-10 predict similar deformed

curvilinear velocity profiles in resemblance to those of the latter except that the fluid accelerates as  $Gr$ ,  $\phi_1$ ,  $\phi_2$  and  $Br$  increase but slightly as per the Stark number  $N$  and  $Fs$ . The dimensionless temperature plots against the dimensionless transverse distance is depicted in Figures 11-17, the fluid temperature in substrate and clear fluid regions rises when each of the parameters  $Gr$ ,  $Br$ ,  $N$  and  $\sigma$  is increased as per Figures 11-14 while Figures 15-17 unveil rapid fall in temperature, and consequently a reduction in the thermal boundary layer prevails as the permeability and thermal conductivity ratios, and substrate thickness increase in values. Also increase in the Forchheimer number consequently features a little fall in temperature (not shown due to space economy).

## 5. Conclusions

Adomian decomposition method (ADM) has been employed to investigate the heat and momentum transfer for an electrically conducting fluid streaming in a vertical channel whose one of its parallel walls is perfectly attached a porous substrate of definite width while the other wall has been subjected to a prescribed wall temperature in the presence of a uniform transverse magnetic field. Introducing new dimensionless variables alongside a similarity variable, the governing PDEs together with the fluid-substrate and wall boundary conditions are reduced to ODEs and then solved via ADM with Maple 18 written scripts for implementing the numerical simulations. Our findings reveal among others the following:

- Skin-friction coefficients and surface heat transfer rates increase in magnitudes when Brinkman, Grashof and numbers as well as conductivity ratio strengthen for low range Forchheimer number but they all reduce in values for strengthening substrate thickness parameter as well as large range of Forchheimer numbers.
- Both wall surface shear parameters reduce absolutely as the permeability parameter intensifies. On the other hand, the heat transfer rates at the walls increase with permeability parameter, Brinkman and Grashof numbers. Nusselt numbers and skin-friction coefficients all reduce values as the permeability ratio  $\phi_1$  increases while skin-friction coefficients as well as the Nusselt numbers can be increased due to intensification of the radiation parameter or Stark number.
- Both substrate thickness parameter and Forchheimer number impede the fluid velocity in either of the porous and clear fluid regions whereas the Brinkman and Grashof numbers, the permeability and conductivity ratios can increase very rapidly velocity in both regions while the Stark and Forchheimer numbers do very slowly.
- The fluid temperature in substrate and clear fluid regions rises when each of the Grashof and Brinkman numbers, radiation and porous medium permeability parameters is increased.

## Figures

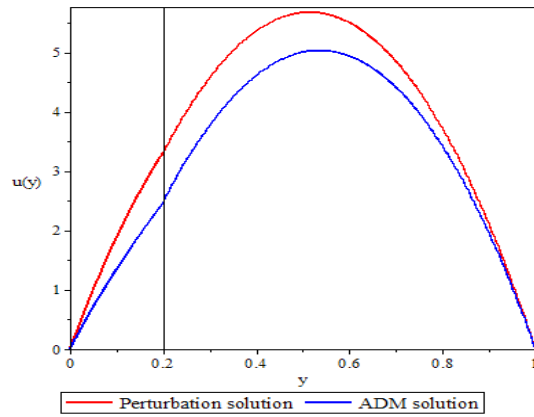


**Figure 2:** Velocity profiles,  $u$  vs.  $y$  for  $F_s = 0$

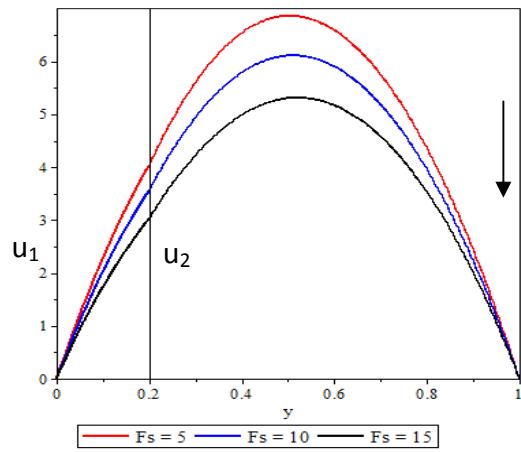


**Figure 3:** Velocity profiles,  $u$  vs.  $y$

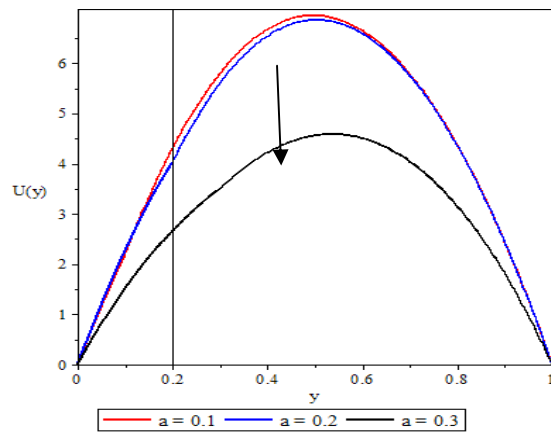


**Figure 4:** Velocity profiles,  $u$  vs.  $y$

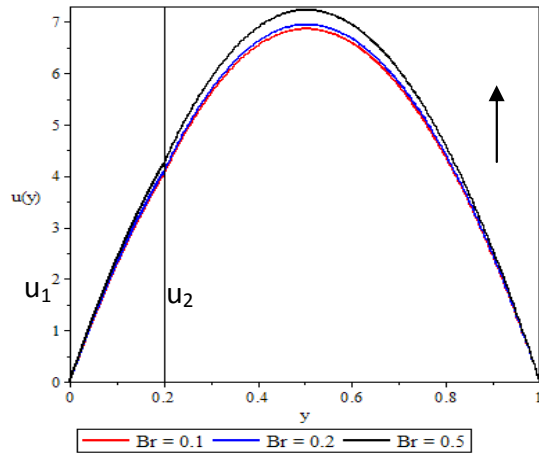


**Figure 5:** Velocity profiles,  $u$  vs.  $y$

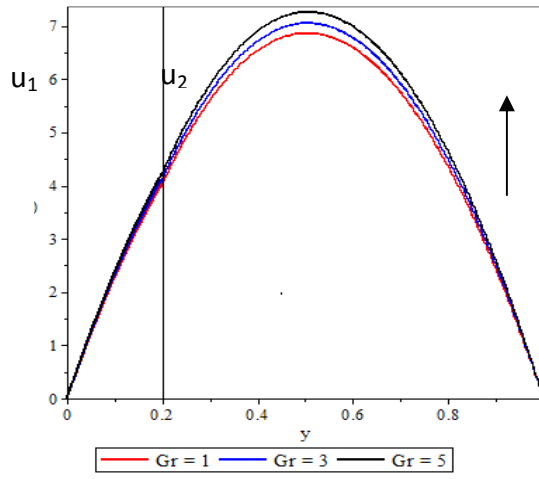


**Figure 6:** Velocity profiles,  $u$  vs.  $y$

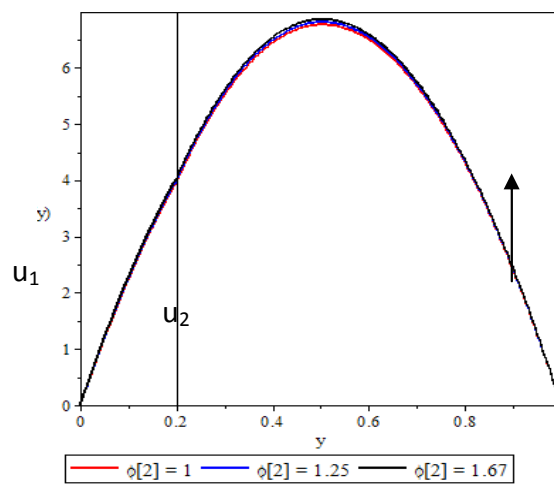


**Figure 7:** Velocity profiles,  $u$  vs.  $y$

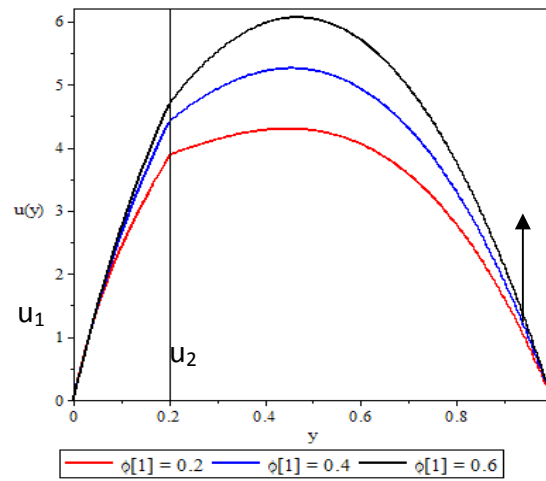


**Figure 8:** Velocity profiles,  $u$  vs.  $y$

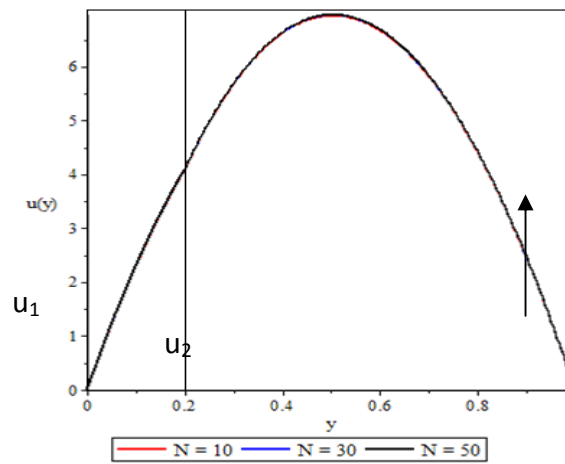


**Figure 9:** Velocity profiles,  $u$  vs.  $y$

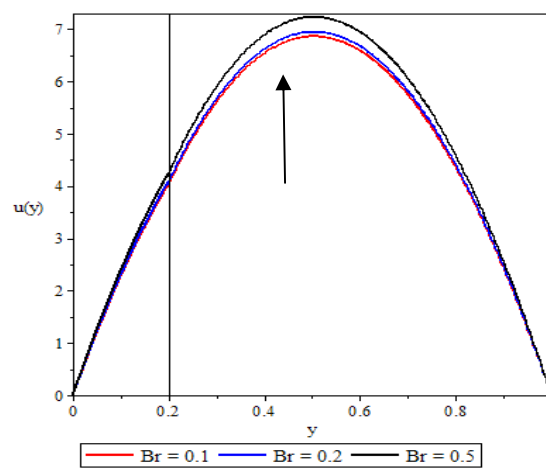


**Figure 10:** Velocity profiles,  $u$  vs.  $y$

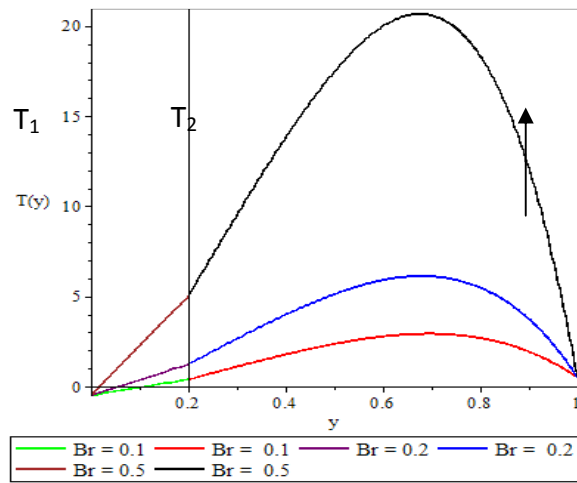


Figure 11: Temperature profiles,  $T$  vs.  $y$

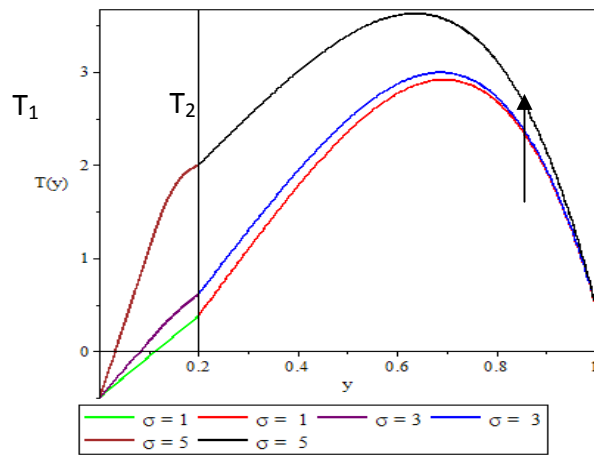


Figure 12: Temperature profiles,  $T$  vs.  $y$

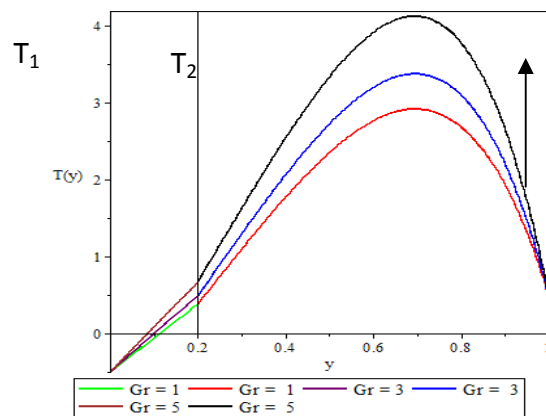
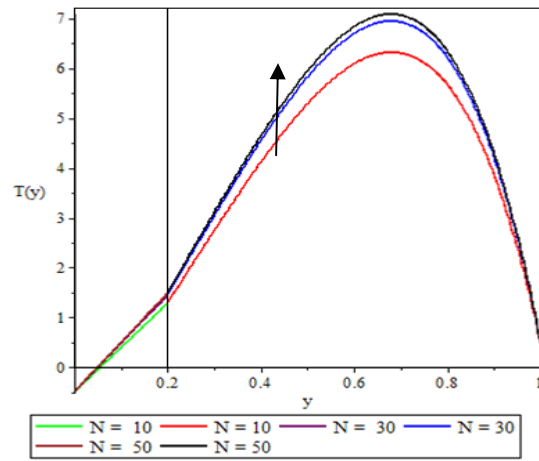
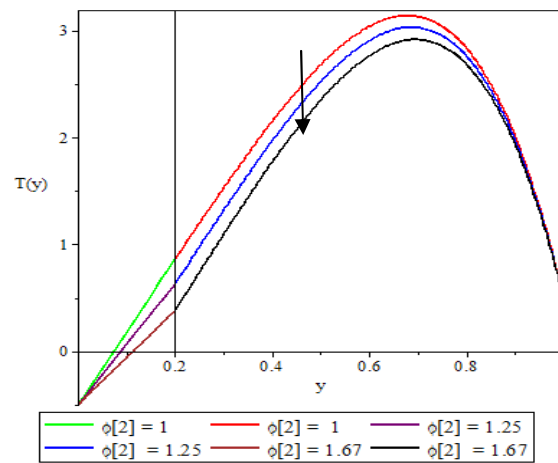


Figure 13: Temperature profiles,  $T$  vs.  $y$



**Figure 14:** Temperature profiles,  $T$  vs.  $y$



**Figure 15:** Temperature profiles,  $T$  vs.  $y$

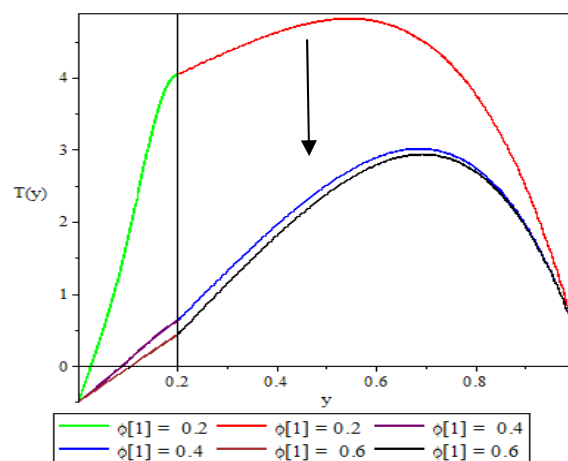


**Figure 16:** Temperature profiles,  $T$  vs.  $y$

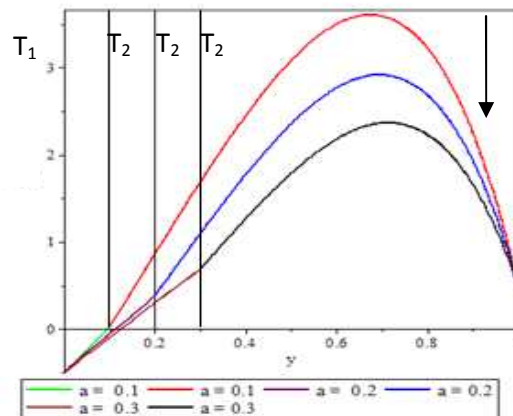


**Figure 17:** Temperature profiles,  $T$  vs.  $y$

**Acknowledgments:** One of the authors A.A, wishes to thank the University of Lagos for provision of books, referred articles and computer facilities. Also, their gratitude goes to the unknown reviewers for their tangible suggestions and corrections.

## References

- [1] D.B. Ingham and I. Pop, *Transport Phenomena in Porous Media*, Elsevier, Oxford, UK, (2005).
- [2] D.A. Nield and A. Bejan, *Convection in Porous Media (3<sup>rd</sup> Ed.)*, Springer Science + Business Media, Inc., New York, (2006).
- [3] S. Ostrach, Combined natural- and forced-convection laminar flow and heat transfer of fluids with and without heat sources in channels with linearly varying wall temperatures, *NACA, Technical Note*, 3141(1954), 1-74.
- [4] C. Beckermann, S. Ramadhyani and R. Viskanta, Natural convection flow and heat transfer between a fluid layer and a porous layer inside a rectangular enclosure, *J. of Heat Transfer*, 109(1987), 363-370.
- [5] A. Barletta, Heat transfer by fully developed flow and viscous heating in a vertical channel with prescribed wall heat fluxes, *Int. J. of Heat Transfer*, 42(1998), 3873-3885.
- [6] J.A. Chamkha, On laminar hydromagnetic mixed convection flow in a vertical channel with symmetric and asymmetric wall heating conditions, *Int. J. of Heat and Mass Transfer*, 45(2002), 2509-2525.
- [7] O.D. Makinde and E. Osalusi, MHD steady flow in a channel with slip at the permeable boundaries, *Rom. Journ. Phys., Bucharest*, 51(3-4) (2005), 319-328.

- [8] A.S. Eegunjobi and O.D. Makinde, Combined effect of buoyancy force and Navier slip on entropy generation in a vertical porous channel, *Entropy*, 14(2012), 1028-1044.
- [9] S. Khamis, O.D. Makinde and Y. Nkansah-Gyekye, Modelling the effects of variable viscosity in unsteady flow of nanofluids in a pipe with permeable wall and convective cooling, *Applied and Computational Mathematics*, 3(3) (2014), 75-84.
- [10] A. Adeniyani and J.A. Adigun, Transient MHD boundary-layer slip-flow of heat and mass transfer over a stretching surface embedded in porous medium with waste discharge concentration and convective boundary conditions, *Applied and Computational Mathematics*, 3(5) (2014), 247-255.
- [11] D.S. Chauhan and V. Kumar, Effects of slip conditions on forced convection and entropy generation in a circular channel occupied by a highly porous medium: Darcy extended Brinkman-Forchheimer model, *Turkish J. Eng. Env. Sci.*, 33(2009), 91-104.
- [12] R. Siegel and J.R. Howell, *Thermal Radiation Heat Transfer (3<sup>rd</sup> Ed.)*, Hemisphere Publishing Corporation, Washington D.C., USA, (1992).
- [13] T. Grosan and I. Pop, Thermal radiation effect on fully developed mixed convection flow in a vertical channel, *Technische Mechanik*, 27(1) (2007), 37-47.
- [14] C. Israel-Cookey, V.B. Omubo-Pepple and I. Tamunobereton-Ari, On steady hydromagnetic flow of a radiating viscous fluid through a horizontal channel in a porous medium, *American J. of Scientific and Industrial Research, Sci. Huß*, 1(2) (2010), 303-308.
- [15] D.S. Chauhan and P. Rastogi, Radiation effects on natural convection MHD flow in a rotating vertical porous channel partially filled with a porous medium, *Applied Math. Sci.*, 4(13) (2010), 643- 655.
- [16] N.C. Jain, D. Chaudhary and H. Singh, Three dimensional radiative heat and mass transfer periodic flow through a vertical porous channel with transpiration cooling and slip boundary conditions, *Appl. Math.*, 3(3) (2013), 71-92.
- [17] A.J. Chamkha, Flow of two immiscible fluids in porous and nonporous channels, *J. of Fluids Engng., ASME*, 122(2000), 117-124.
- [18] M.M.S. El-Din, Effect of viscous dissipation on laminar mixed convection in a horizontal double-passage channel with uniform wall heat flux, *Int. J. of Therm. Sci.*, 41(2002), 787-794.
- [19] M.M.S. El-Din, Laminar fully developed mixed convection with viscous dissipation in a uniformly heated vertical double-passage channel, *Int. J. of Therm. Sci.*, 11(1) (2007), 27-41.
- [20] T.V.A.P. Sastry, M.V. Krishna, S. Sreenadh and M.V. Ramanamurthy, Couette flow of two immiscible fluids between two permeable beds, *ARPN J. of Eng. Appl. Sci.*, 5(2) (2010), 78-81.
- [21] O.D. Makinde and P.Y. Mhone, Heat transfer to MHD oscillatory flow in a channel filled with porous medium, *Rom. Journ. Phys., Bucharest*, 50(9-10) (2005), 931-938.

- [22] M.M. Hamza, B.Y. Isah and H. Usman, Unsteady heat transfer to MHD oscillatory flow through a porous medium under slip condition, *Int. J. of Computer Applications*, 33(4) (2011), 12-17.
- [23] S.O. Adesanya and O.D. Makinde, MHD oscillatory slip flow and heat transfer in a channel filled with porous media, *U.P.B. Sci. Bull., Series A*, 76(1) (2014), 197-204.
- [24] D.S. Chauhan and R. Agrawal, MHD flow and heat transfer in a channel bounded by a shrinking sheet and a porous medium bed: Homotopy analysis method, Hindawi Publishing Corporation, *ISRN Thermodynamics*, 2013(nil) (2013), 1-10.
- [25] M. Narahari, Transient free convection flow between two long vertical parallel plates with constant temperature and mass diffusion, *Proceedings of the World Congress on Engineering*, WCE-2008, London, U.K, ISBN, 2(2008), 978-988.
- [26] U.S. Rajput and P.K. Sahu, Combined effect of MHD and radiation on unsteady transient free convection flow between two long vertical parallel plates with constant temperature and mass diffusion, *Gen. Math. Notes*, 6(1) (2011), 25-39.
- [27] U.S. Rajput and P.K. Sahu, Transient free convection MHD flow between two long vertical parallel plates with variable temperature and uniform mass diffusion in a porous medium, *ARPJ. J. of Eng. and Appl. Sci.*, 6(8) (2011), 79-86.
- [28] K.D. Singh, MHD mixed convection visco-elastic slip flow through a porous medium in a vertical porous channel with thermal radiation, *Kragujevac J. Sci.*, 35(2013), 27-40.
- [29] D.S. Chauhan and V. Kumar, Radiation effects on mixed convection flow and viscous heating in a vertical channel partially filled with a porous medium, *Tamkang J. of Sci. and Eng.*, 14(2) (2011), 97-106.
- [30] G. Adomian, *Solving Frontier Problems of Physics, the Decomposition Methods*, Kluwer Academic Press, Dordrecht, (1994).
- [31] A. Wazwaz, *Partially Differential Equations and Solitary Waves Theory*, Higher Education Press, Beijing and Springer-Verlag Berlin Heidelberg, (2001).
- [32] H. Mirgolbabaei, A. Barari, L.B. Ibsen and M.G. Esfahani, Analytic solution of forced-convective boundary-layer flow over a flat plate, *Archives of Civil and Mech. Engng.*, 10(2) (2010), 42-51.
- [33] N.F.M. Noor, S.A. Kechil and I. Hashim, Simple non-perturbative solution for MHD viscous flow due to a shrinking sheet, *Commun Nonlinear Sci Numer Simulat*, 15(2) (2010), 144-148.
- [34] O.D. Makinde, B.I. Olajuwon and A.W. Gbolagade, Adomian decomposition approach to a boundary layer flow with thermal radiation past a moving vertical porous plate, *Int. J. of Appl. Math and Mech.*, 3(3) (2007), 62-70.
- [35] T. Chinyoka and O.D. Makinde, Analysis of entropy generation rate in an unsteady porous channel flow with Navier slip and convective cooling, *Entropy*, 15(2013), 2081-2099.

- [36] H. Heidarzadeh, M.M. Joubari and R. Asghari, Application of adomian decomposition to nonlinear heat transfer equation, *J. of Math. and Comp. Sci.*, 4(3) (2012), 436-447.
- [37] J.P. Kumar, J.C. Umavathi and Y. Ramarao, Free and forced convective flow in a vertical channel filled with composite porous medium using Robin boundary conditions, *American J. of Appl. Math.*, 2(4) (2014), 96-110.
- [38] B. Bellomo and R. Monaco, A comparison between Adomian's decomposition methods and perturbation techniques for nonlinear random differential equations, *J. Math. Anal. Appl.*, 110(1985), 495-502.
- [39] R. Rach, On the adomian decomposition method and comparisons with Picard's method, *J. Math. Anal. Appl.*, 128(1987), 480-483.
- [40] H. Saleh and I. Hashim, Flow reversal of fully-developed mixed MHD convection in vertical channels, *Chin. Phys. Lett.*, 27(2) (2010), 024401\_1-024401\_3.
- [41] A. Barletta and E. Zanchini, On the choice of reference temperature for fully developed mixed convection in a vertical channel, *Int. J. Heat Mass Transfer*, 42(1999), 3169-3181.
- [42] Y.Q. Hasan and L.M. Zhu, Modified adomian decomposition method for singular initial value problems in the second order ordinary differential equations, *Surveys in Math. and Appl.*, 3(2008), 183-193.